

# Investigation on Micro-abrasive Jet Machining: Machinability Study

Kumar Abhishek, Somashekhar S. Hiremath\*

Department of Mechanical Engineering, Indian Institute of Technology Madras, Chennai, India

## Email address

abhilbra90@gmail.com (K. Abhishek), somashekhar@iitm.ac.in (S. S. Hiremath)

\*Corresponding author

## To cite this article

Kumar Abhishek, Somashekhar S. Hiremath. Investigation on Micro-abrasive Jet Machining: Machinability Study. *American Journal of Materials Science and Application*. Vol. 5, No. 2, 2017, pp. 9-15.

**Received:** May 30, 2017; **Accepted:** July 6, 2017; **Published:** August 17, 2017

## Abstract

Micro-Abrasive Jet Machining ( $\mu$ -AJM) is an advanced mechanical micromachining process used to machine various engineering materials - brittle and ductile. The paper presents a study on machinability of brittle material as Sodalime glass and Quartz glass and ductile material as Polymethyl Methacrylate (PMMA) through  $\mu$ -AJM. Three different commercial abrasives – Aluminium Oxide ( $\text{Al}_2\text{O}_3$ ), Silicon Carbide (SiC), and Synthetic Diamond (C) of has been employed to impact three different workpiece materials. Machinability of materials after different abrasives impact is compared in terms of Material Removal Rate (MRR) and surface morphology. The study revealed that the type of abrasive and their hardness along with the fracture toughness of the workpiece are significant factors determining the machinability of workpiece material in  $\mu$ -AJM. Synthetic Diamond abrasive gives maximum material removal rate irrespective of workpiece materials used whereas the best surface morphology is obtained with Aluminium Oxide abrasive.

## Keywords

Material Removal Rate, Surface Morphology, Brittle Material, Ductile Material

## 1. Introduction

$\mu$ -AJM is an advance mechanical micromachining process in which the material is removed from the workpiece irrespective of their size in the form of chips having the size range of  $1\mu\text{m}$  -  $999\mu\text{m}$ . In  $\mu$ -AJM abrasive particles size is in the range of  $10\mu\text{m}$  -  $100\mu\text{m}$  and the nozzle diameter is less than 1 mm. The material removal mechanism of  $\mu$ -AJM has been derived from the theories of solid particle impact erosion of surfaces. The erosion due to solid particle impact is classified based on the two types of material behaviour brittle and ductile [1]. The brittle erosion is due to the propagation and intersection of cracks leading to fracture of the material and the ductile erosion takes place due to plastic deformation and cutting action of the particle. At low impact angle of the solid particle, ductile erosion is dominant whereas at normal impact brittle erosion dominates [2].

The process and its application have evolved from a rough working operation like surface cleaning, scale and paint

removal to precision machining of micro sized features, employed in the microfabrication of micro devices. Researchers have constantly contributed to the evolution and development of the process through their various interesting research findings. The effect of factors such as Nozzle Stand-off Distance (NSD), air pressure, abrasive size, and mixture ratio on MRR, penetration rate and diameter of the cavity machined on the glass have been studied. The MRR and penetration rate increases when NSD increase upto 16 mm and 7 mm respectively to their maximum and then decreases when NSD is increased further beyond 16 mm and 7 mm respectively. The diameter of the cavity also increases on increasing NSD. The MRR increases with air pressure up to the certain limit and then saturate [3]. The material response of Alumina ceramic on the impact of three different abrasives Aluminum Oxide ( $\text{Al}_2\text{O}_3$ ), Silicon Carbide (SiC), and Synthetic Diamond (C) has been investigated. The hardness and type of the abrasive particles used were found to be important parameters for machinability study [4]. Sodalime glass has been machined using hot air as carrier media in  $\mu$ -

AJM. An optimum factor setting as NSD 4 mm, feed rate 20 mm/min and air temperature 320°C has been obtained using Taguchi robust design analysis for maximum MRR and minimum surface roughness. An increase in MRR and decrease in surface roughness with an increase in air temperature has been reported [5]. By integrating the AJM set-up with a fluidized bed mixing chamber and pressurized powder feeding system k-99 alumina ceramic has been machined. The effect of input parameters such as air pressure, NSD and abrasive grain size on the responses such as MRR, surface roughness, depth of cut, taper angle, overcut and flaring diameter have been studied by establishing quadratic regression model and optimized the parameters using particle swarm optimization. The optimized parametric setting obtained is air pressure 5 bar, NSD 8 mm and abrasive grain size 260 μm [6]. A model has been developed to predict the MRR of glass. The MRR was found to increase with the increase in the nozzle diameter and abrasive particle size [7]. A theoretical model has been developed to study the abrasive particle velocity. As air pressure increases the particle velocity at nozzle exit increases. The centerline particle velocity increases beyond nozzle exit along axial distance up to a distance at which the air flow velocity and particle velocity becomes equal and beyond that, it decreases [8]. A semi-empirical model has been developed to study the shape of the surface generated in the μ-AJM. It was observed that the machined surface is conical in shape with an edge radius at the entry side of the target surface [9]. A novel approach to improve the geometrical accuracy of the machined micro holes through the μ-AJM process has been presented. In the new approach NSD is maintained constant during machining which results in reduced taper angle of the hole by approximately 58% [10]. Micro channels - 100 μm wide and 30 μm deep have been machined on the sodalime glass for microfluidic bio-analytical applications [11]. A ball valve micropump using borosilicate glass has been fabricated

through the μ-AJM process. A conical shaped hole of diameter 700 μm was employed to function as a ball valve seat [12]. Micro channels of 200 μm width × 170 μm depth × 24 mm length have been machined on glass for the fabrication of a micro direct methanol fuel cell [13].

μ-AJM has been used effectively to machine brittle materials like glass and ceramics [14, 15]. Many researchers have also machined soft and ductile materials like various composites and polymeric materials - PMMA [16], Polycarbonate [17], Polypropylene [18], bismaleimide polymers [19], quartz-polyimide, glass-epoxy and quartz-polybutadiene composites [20], etc.

Machinability of brittle and ductile materials through μ-AJM is still not clear. Therefore in the present work, a comprehensive study comparing the machinability of the brittle and ductile has been presented.

## 2. Materials and Method

Machinability study of brittle and ductile material on different abrasive particles impact is carried out. The factors involved are workpiece materials and abrasives employed for impact. Both these factors are categorical factors. The type of workpieces, abrasives used and their material properties are mentioned in the subsection given below

### 2.1. Materials

Glass and PMMA are the important materials employed for the microfabrication of microfluidic chips due to their excellent optical transparency and chemical inertness. Therefore in the current investigation Glass - Sodalime glass plate and Quartz glass plate and Polymer - PMMA plate of thickness 2 mm are selected as workpieces. Some of the important material properties of these workpieces are listed in Table 1.

Table 1. Properties of workpiece material.

Properties	Sodalime	Quartz	PMMA
Density (kg/m <sup>3</sup> )	2440	2220	1150 - 1190
Hardness	585 (Knoop hardness kg/mm <sup>2</sup> )	820 (Knoop hardness kg/mm <sup>2</sup> )	90 – 99 (Shore D)
Fracture toughness (MPa m <sup>1/2</sup> )	0.7 - 0.8	0.75	0.7 - 1.6

Glass is hard and brittle in nature whereas polymers like PMMA are soft and ductile in nature. The hardness and the fracture toughness of these materials have an inverse correlation, can be referred from the table that fracture toughness for PMMA (soft and ductile) is more compared to the glass (hard and brittle).

Three different type of abrasives - Aluminium Oxide (Al<sub>2</sub>O<sub>3</sub>), Silicon Carbide (SiC), and Synthetic Diamond (C) of abrasive mesh #320 are selected for experimentation. Out of three, the first two are the commonly used abrasives in abrasive machining processes and the third one is a super abrasive as it is the hardest abrasive known. Table 2 lists some properties of the abrasives used.

Table 2. Properties of abrasives.

Properties	Al <sub>2</sub> O <sub>3</sub>	SiC	C
Density (kg/m <sup>3</sup> )	3690	3100	3900
Knoop hardness (kg/mm <sup>2</sup> )	2100	2480	7000
Fracture toughness (MPa m <sup>1/2</sup> )	3.5	4.6	13

### 2.2. Methods

MRR and surface morphology of the impacted workpiece surface has been considered as responses in the present experiment. Here, MRR is a quantitative response measured in mg/min by dividing the difference in weight (mg) of the workpiece before and after machining with machining time

(s). The surface morphology of the workpiece surface impacted by the abrasives is the qualitative response.

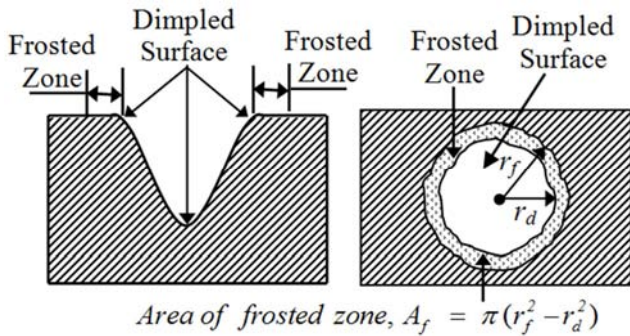


Figure 1. Schematic representation of dimpled surface and frosted zone.

Surface morphology of the three workpieces impacted by the different abrasives has been discussed in terms of their frosted zone and dimpled surface. The frosted zone is described as a region in which the workpiece surface is just indented by the abrasive particles with very small fracture or chipping of material around the periphery of the dimple. These frosted zones are caused by the abrasive particles at

the periphery of the abrasive air jet which do not have sufficient energy to fracture the workpiece surface and just produce an indentation mark at the workpiece surface on impact with very little chipping of material. It can be avoided using the mask as it can confine the area over the workpiece surface to be impacted by the abrasive particles. Figure 1 shows the schematic representation of dimpled surface and frosted zone. The evaluation of frosted zone area ( $A_f$ ) similar to an annulus area is shown in Figure 1.

### 3. Experimentation

Figure 2 shows the  $\mu$ -AJM experimental setup developed based on the basic principles. The main components of the setup are an air cylinder, abrasive canister to hold the abrasive, nozzle, filter and regulator unit to remove the moisture from the compressed air, 3/2 solenoid valve to start and stop the machining, pressure gauges to monitor the pressure in the pneumatic lines. The developed setup is capable of machining various features on different engineering materials by varying factors involved in the process.

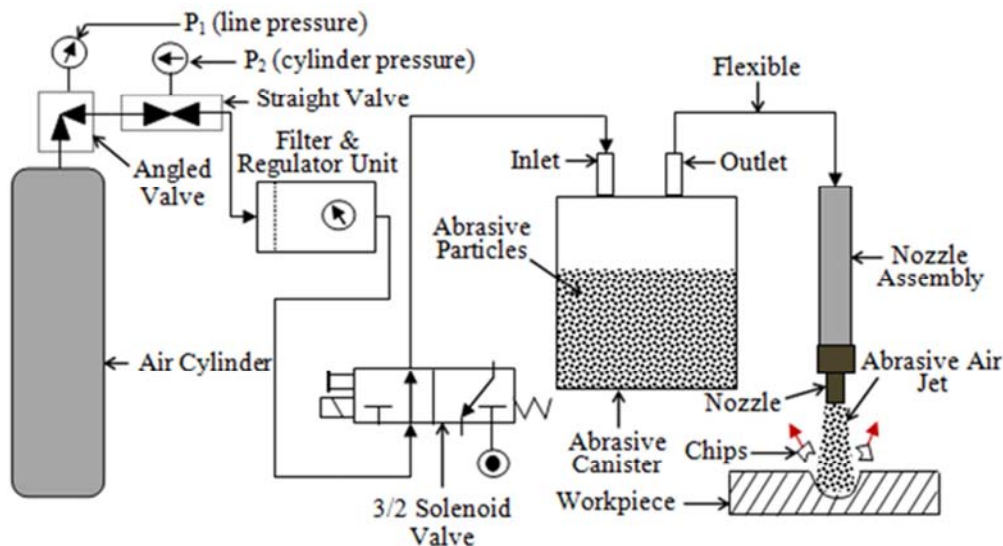


Figure 2. Schematic diagram of developed  $\mu$ -AJM experimental setup.

In the current experiment, only two categorical factors – workpiece material and abrasive type are changed keeping all other factors constant. Factors like abrasive mesh, air pressure, NSD, etc. have been kept constant and are listed in Table 3.

Table 3. Constant factors for machinability study.

Factors	Values
Abrasive mesh (no units)	#320
Air pressure	6 bar
Nozzle stand-off distance	2 mm
Nozzle diameter	0.896 mm
Machining time	10 s
Impact angle	90°

A full factorial design for two categorical factors at three

levels gives a total of nine experimental runs ( $3^k = 3^2 = 9$ ). Each run has different combination levels of the factors. Table 4 shows the full factorial design layout for machinability study.

Table 4. Full factorial design layout for machinability study.

Exp. Runs	Workpieces	Abrasives
1	Sodalime glass	Al <sub>2</sub> O <sub>3</sub>
2	Sodalime glass	SiC
3	Sodalime glass	C
4	Quartz glass	Al <sub>2</sub> O <sub>3</sub>
5	Quartz glass	SiC
6	Quartz glass	C
7	PMMA	Al <sub>2</sub> O <sub>3</sub>
8	PMMA	SiC
9	PMMA	C

### 4. Results and Discussions

Machinability is defined as the ease with which the material can be cut and removed from the workpiece with a cutting tool. In  $\mu$ -AJM, the abrasive particles act as a tool and can be used only once because they lose their cutting edge on impact and get mixed with chipped workpiece material. Therefore reuse of abrasives mixed with chipped workpiece materials may clog the nozzle. In  $\mu$ -AJM machinability of the materials has been discussed in terms of MRR and surface morphology of the worksurface.

#### 4.1. Material Removal Rate

Figure 3 shows the SEM images of different workpieces impacted with different abrasives. Three different type of workpieces – Sodalime glass plate, Quartz glass plate and PMMA plate of thickness 2 mm have been impacted for 10 s by three different abrasives – Aluminium Oxide ( $Al_2O_3$ ), Silicon Carbide (SiC), and Synthetic Diamond (C) of #320 abrasive mesh. A clear dimple of appreciable depth can be observed in Sodalime glass plate and Quartz glass plate visually from the Figure 3 but not clearly defined dimple in PMMA plates. The reason for this is due to high fracture toughness of the PMMA plate as compared to the glass plate.

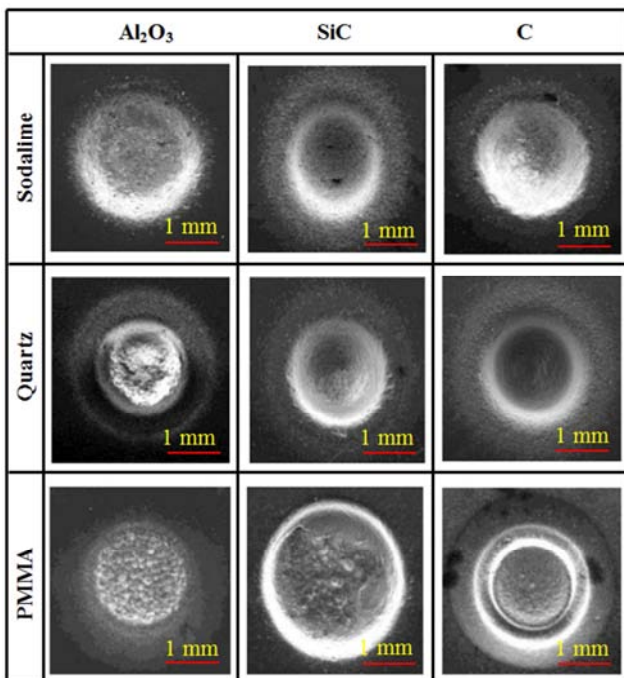


Figure 3. SEM images of different workpieces impacted with different abrasives.

Figure 4 shows the MRR for different workpiece materials impacted with different abrasives. For every experimental run, the experiment is repeated three times and the mean value of the MRR evaluated is shown in Figure 4. The MRR deviation of the repeated experiment from the mean value of MRR was found to be less than 3% which shows repeatability of the process. Out of three abrasives used -

Aluminium Oxide, Silicon Carbide and Synthetic Diamond, MRR has been observed maximum for Synthetic Diamond then for Silicon Carbide and minimum for Aluminium Oxide in all the three workpieces. This is due to the high hardness of Synthetic Diamond abrasive ( $7000 \text{ kg/mm}^2$ ) as compared to Silicon Carbide ( $2480 \text{ kg/mm}^2$ ) and Aluminium Oxide ( $2100 \text{ kg/mm}^2$ ). On comparing the MRR obtained with each abrasives for all three workpiece it has been found that there is no significant difference in MRR of two different types of glass plates i.e. Sodalime and Quartz obtained with same abrasive, whereas a significant difference in MRR of PMMA compared to both the glass has been observed in case of same abrasive.

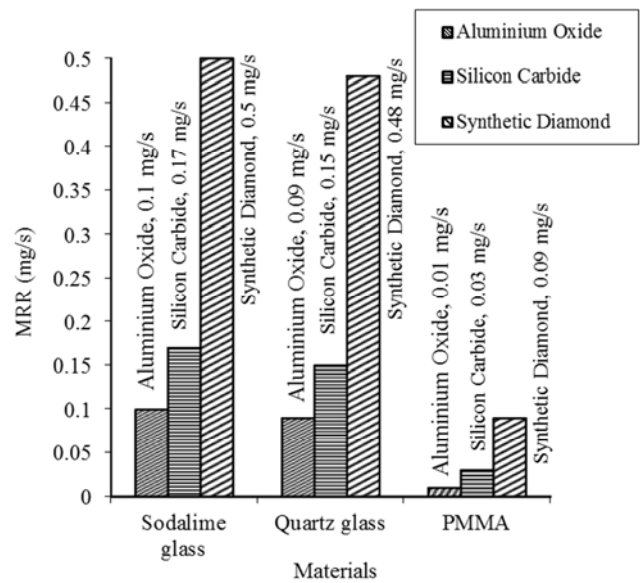


Figure 4. MRR for different workpiece materials impacted with different abrasives.

The reason for the insignificant difference in MRR of glass plates with same abrasive impact is due to similar brittle nature of the material and their comparable fracture toughness of  $0.7 - 0.8 \text{ MPa m}^{1/2}$  for Sodalime and  $0.75 \text{ MPa m}^{1/2}$  for Quartz. However, the significant difference in MRR of PMMA compared with glass is due to its ductile nature and high fracture toughness of  $0.7 - 1.6 \text{ MPa m}^{1/2}$  as compared to glass. This implies that the abrasives type, their hardness and fracture toughness of the workpiece are the most significant parameters for the machinability in the  $\mu$ -AJM process.

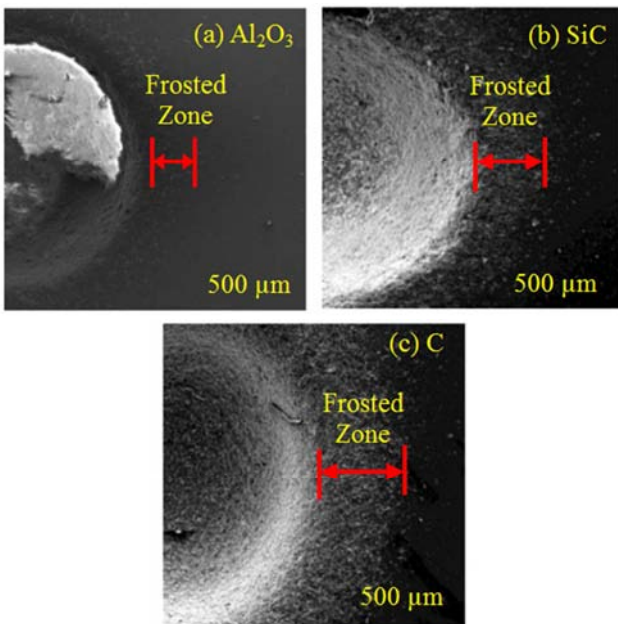
#### 4.2. Surface Morphology

Table 5 lists the area of the frosted zone on different workpiece impacted with different abrasives. It can be observed from the Table 5 that the maximum of the area of the frosted zone ( $A_f$ ) on every workpiece occurs in the case of Synthetic Diamond, then in the case of Silicon Carbide and minimum in case of Aluminium Oxide. The area of the frosted zone should be minimum as it affects the surface integrity of the machined workpiece surface.

**Table 5.** Area of frosted zone on different workpiece impacted with different abrasives.

Workpieces	Area of frosted zone, $A_f$		
	$Al_2O_3$	SiC	C
Sodalime glass plate	0.58 mm <sup>2</sup>	1.53 mm <sup>2</sup>	4.28 mm <sup>2</sup>
Quartz glass plate	2.51 mm <sup>2</sup>	2.62 mm <sup>2</sup>	4.84 mm <sup>2</sup>
PMMA plate	0.62 mm <sup>2</sup>	0.71 mm <sup>2</sup>	2.70 mm <sup>2</sup>

Figure 5 shows SEM images of the frosted zone on Sodalime glass plate impacted with different abrasives. It can be seen from the Figure 5 that the frosted zone in case of Aluminium Oxide abrasive impact is very less as compared to the Silicon Carbide and Synthetic Diamond. Also, the area of the frosted zone on Sodalime glass plate in case of Aluminium Oxide is 0.58 mm<sup>2</sup> which is less compared to 1.53 mm<sup>2</sup> in the case of Silicon Carbide and 4.28 mm<sup>2</sup> in the case of Synthetic Diamond.



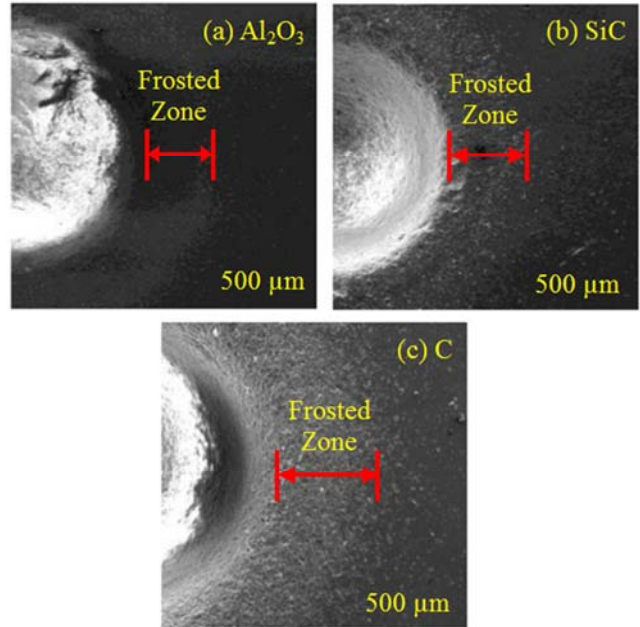
**Figure 5.** SEM images of the frosted zone on sodalime glass plate impacted with different abrasives.

The area of the frosted zone in case of Synthetic Diamond is more as compared to the Silicon Carbide and Aluminium Oxide. The indentations in frosted zone caused by Synthetic Diamond abrasive particles appear to be deeper compared to those caused by other abrasive particles.

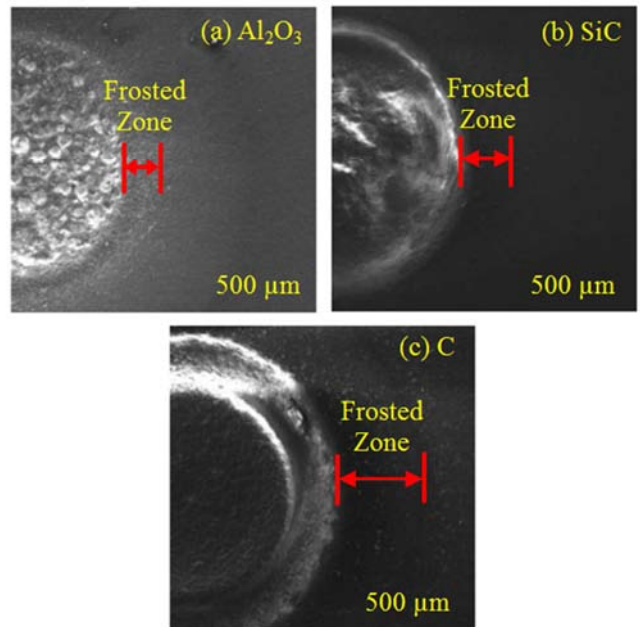
Figure 6 shows SEM images of the frosted zone on Quartz glass plate impacted with different abrasives. The indentation depths of the abrasives in the frosted zone in Quartz glass plates appear to be less as compared to those in the case of the Sodalime glass sample.

This is due to the higher hardness of the Quartz glass plate (820 kg/mm<sup>2</sup>) as compared to the Sodalime glass plate (585 kg/mm<sup>2</sup>) and hence former offers greater resistance to the abrasive impacts than the latter. The area of the frosted zone on Quartz glass plate in case of Aluminium Oxide is 2.51 mm<sup>2</sup> which is less compared to 2.62 mm<sup>2</sup> in the case of Silicon Carbide and 4.84 mm<sup>2</sup> in the case of Synthetic

Diamond. From Figure 6 it can be observed that the indentations are deeper in frosted zone caused by Synthetic Diamond abrasive particles as compared to those caused by the Aluminium Oxide abrasive particles and Silicon Carbide abrasive particles due to its higher hardness compared to Aluminium Oxide and Silicon Carbide abrasives. The glass plate impacted by the Aluminium Oxide has a less dense frosted zone in comparison to the other two glass plates.



**Figure 6.** SEM images of the frosted zone on quartz glass plate impacted with different abrasives.



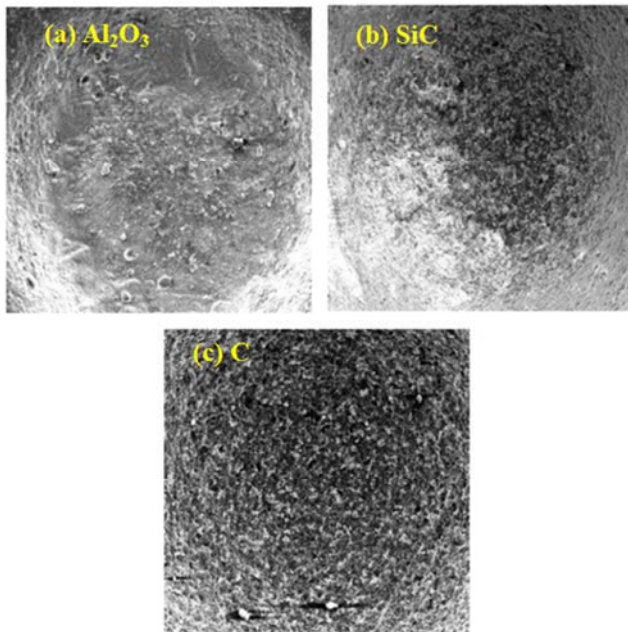
**Figure 7.** SEM images of the frosted zone on PMMA plate impacted with different abrasives.

Figure 7 shows SEM images of the frosted zone on PMMA plate impacted with different abrasives. PMMA polymer is a soft material and has high fracture toughness

compared to glass. Therefore PMMA plates on abrasive particles impacts absorb the greater fraction of the impact energy of the impacting abrasive particles than that absorbed by the glass plates. The area of the frosted zone on PMMA plate in case of Aluminium Oxide is  $0.62 \text{ mm}^2$  which is less compared to  $0.71 \text{ mm}^2$  in the case of Silicon Carbide and  $2.70 \text{ mm}^2$  in the case of Synthetic Diamond.

Due to high fracture toughness of PMMA plates than glass plates the impacting abrasive particles at the periphery of the abrasive air jet indent the PMMA plates less compared to glass plates and results in a very less indentation and chipping in the frosted zones on the PMMA plates than those in the glass plates. It can be noticed from Figure 7 that the density of the frost in the case of the PMMA plates is very less as compared to that of glass plates.

Figure 8 shows SEM images of the dimpled surface on Sodalime glass plate impacted with different abrasives.



**Figure 8.** SEM images of the dimpled surface on sodalime glass plate impacted with different abrasives.

The dimpled surface produced after abrasives impact appears to be rough from Figure 8. It can be observed that the surface produced by the Aluminium Oxide abrasive impact are less rough compared to the surfaces produced by Silicon Carbide and Synthetic Diamond abrasive impacts. The surface produced by the Synthetic Diamond appears to be rougher compared to Silicon Carbide because of greater indentation depth and chipping of materials caused by the Synthetic Diamond abrasive particles due to its high hardness compared to Silicon Carbide abrasive particles.

Figure 9 shows SEM images of the dimpled surface on Quartz glass plate impacted with different abrasives. The dimpled surface on Quartz glass plate appears similar to the dimpled surface on Sodalime glass plates. The dimpled surface produced by the synthetic diamond is the roughest compared to Aluminium Oxide and Silicon Carbide produced

surfaces. The dimpled surface produced by the Aluminium Oxide particles appears to be smooth as compared to the other two surfaces.

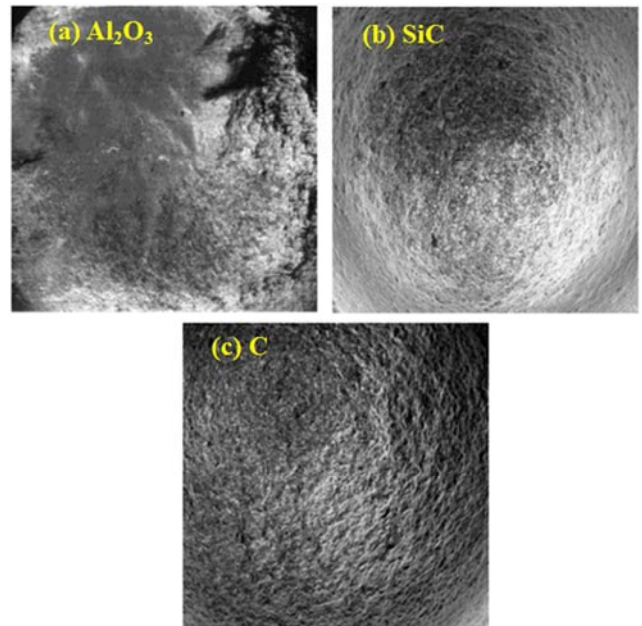


**Figure 9.** SEM images of the dimpled surface on quartz glass plate impacted with different abrasives.

Figure 10 shows SEM images of the dimpled surface on PMMA plate impacted with different abrasives. In the first case, the surface produced by Aluminium Oxide abrasive impacts has very clear scattered indentation of the particles and very minimum material is removed with just leaving the surface rough.

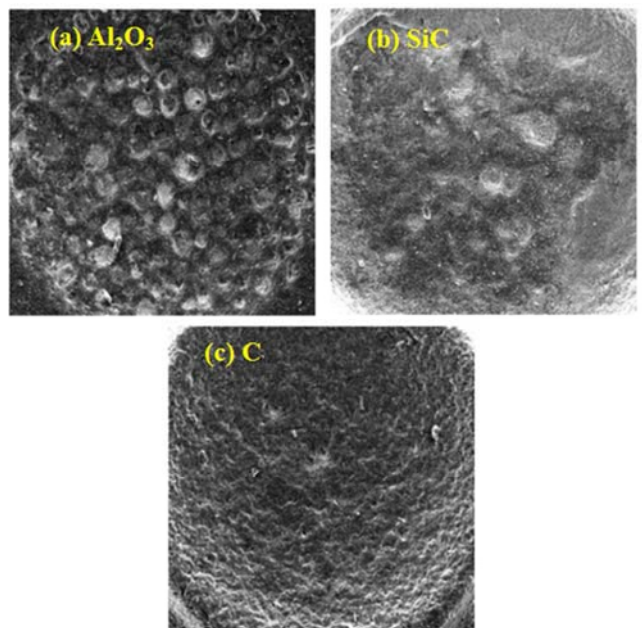


**Figure 10.** SEM images of the dimpled surface on PMMA plate impacted with different abrasives

The Silicon Carbide abrasive particles were able to

fracture the material due to its adequate hardness and new surface produced after material fracture appears to be comparatively smoother than in case surface produced by Aluminium Oxide abrasive impacts. The surface produced by the Synthetic Diamond abrasive impacts is rough as compared to other two surfaces due to deeper indentation and relatively more fracture caused by the Synthetic Diamond particles.

The dimpled surface on PMMA plates appear to be smoother as compared to glass plates for each case of the abrasives impacts because of the different nature of material response of polymer and glass. Glass is hard and brittle and on abrasive impact cracks are formed in median and radial direction and the coalescence of these cracks at the surface results in chipping of the materials from the samples resulting in a rough surface. Whereas, polymers are soft and ductile in nature and go through plastic deformation and flow on impact of the abrasive particles and results in the fracture of the materials and so the surface exposed are less rough than glass due to material flow.

## 5. Conclusions

For both glass and polymer the MRR and surface morphology are greatly influenced by the type of abrasives, their hardness and fracture toughness of the workpiece and therefore these are significant parameters for machinability. Some of the highlights of the investigation are:

- a. For both Sodalime glass plate and Quartz glass plate, the highest MRR has been obtained for Synthetic Diamond (C) abrasive impact, but the surface morphology obtained for all the glass plates impacted by Synthetic Diamond (C) has been found to be poor. The frosted zone and the dimple surface roughness is more for the glass plates impacted by the Synthetic Diamond (C) abrasive whereas minimum for those impacted by the Aluminium Oxide ( $Al_2O_3$ ) abrasive. Therefore for applications where surface morphology and MRR both are important Aluminium Oxide ( $Al_2O_3$ ) should be used as abrasive.
- b. For polymer like PMMA, the trend of MRR for different abrasives impacts was observed to be similar but the dimple surface of the PMMA plates are less rough as compared to the glass plates because of the flow property of the material. The frosted zone observed are also negligible in PMMA plates at the periphery of the dimple but a very light flow of material marks can be observed on PMMA sample at the periphery of the dimple.

## References

- [1] I. Finnie, *Wear*, 1960, 3, 87–103.
- [2] J. G. A. Bitter, *Wear*, 1963, 6, 169–190.
- [3] A. P. Verma and G. K. Lal, *International Journal of Machine Tool Design and Research*, 1984, 24, 19–29.
- [4] M. Wakuda, Y. Yamauchi and S. Kanzaki, *Journal of Materials Processing Technology*, 2003, 132, 177–183.
- [5] N. Jagannatha, S. S. Hiremath and K. Sadashivappa, *International Journal of Mechanical and Materials Engineering*, 2012, 7, 9–15.
- [6] K. Nanda, A. Mishra and D. Dhupal, *International Journal of Advanced Manufacturing Technology*, 2017, 90 (9), 3655–3672.
- [7] A. El-Domiaty, H. M. A. El-hafez and M. A. Shaker, *International Journal of Mechanical, Aerospace, Industrial, Mechatronic and Manufacturing Engineering*, 2009, 32, 61–67.
- [8] H. Z. Li, J. Wang and J. M. Fan, *International Journal of Machine Tools and Manufacture*, 2009, 49, 850–858.
- [9] R. Balasubramaniam, J. Krishnan and N. Ramakrishnan, *Journal of Materials Processing Technology*, 2002, 121, 102–106.
- [10] A. Kumar and S. S. Hiremath, *Procedia CIRP*, 2016, 46, 47–50.
- [11] D. Solignac, A. Sayah, S. Constantin, R. Freitag and M. A. M. Gijs, *Sensors and Actuators, A: Physical*, 2001, 92, 388–393.
- [12] C. Yamahata, F. Lacharme, Y. Burri and M. A. M. Gijs, *Sensors and Actuators, B: Chemical*, 2005, 110, 1–7.
- [13] M. Shen, S. Walter, L. Dovat and M. A. M. Gijs, *Microelectronic Engineering*, 2011, 88, 1884–1886.
- [14] D. Park, M. Cho, H. Lee and W. Cho, *Journal of Materials Processing Technology*, 2004, 146, 234–240.
- [15] J. M. Fan, C. Y. Wang and J. Wang, *Wear*, 2009, 266, 968–974.
- [16] H. Getu, A. Ghobeity, J. K. Spelt and M. Papini, *Wear*, 2007, 263, 1008–1015.
- [17] H. Getu, A. Ghobeity, J. K. Spelt and M. Papini, *Wear*, 2008, 265, 888–901.
- [18] S. M. Walley, J. E. Field and P. Yennadhiou, *Wear*, 1984, 100, 263–280.
- [19] A. Brandstadter, K. C. Goretta, J. L. Routbort, D. P. Groppi and K. R. Karasek, *Wear*, 1991, 147, 155–164.
- [20] J. Zahavi and G. F. J Schmitt, *Wear*, 1981, 71, 179–190.